IMPACT OF LATERAL EFFECTS ON EQE MEASUREMENTS OF LARGE SCALE TANDEM SOLAR CELLS

S. Kasimir Reichmuth[1,2], A. Fell[1,3], G. Siefer[1], M. Schachtner[1], D. Chojniak[1], O. Fischer[1,2], M. Mühleis[1], M. Rauer[1],
J. Hohl-Ebinger[1], M. C. Schubert[1]
[1]Fraunhofer Institute for Solar Energy Systems ISE, Heidenhofstrasse 2, 79110 Freiburg, Germany
Email: kasimir.reichmuth@ise.fraunhofer.de,
[2]Albert-Ludwigs-University, INATECH, Emmy-Noether-Strasse 2, 79110 Freiburg, Germany
[3]AF simulations, Landstr. 33a, 79232 March, Germany

ABSTRACT: Laterally inhomogeneous cell parameters in large scale perovskite/silicon (PSC/Si) tandem solar cells may significantly influence the device performance. The lateral quality of the absorber can be analysed with electroluminescence (EL), photoluminescence (PL) and thermographic methods. In addition to a global impact on cell performance, such lateral effects are often not considered in *EQE* and *I-V*-characterization of tandem devices, yet may lead to erroneous measurement results. Therefore, we see the necessity to employ large-area 3D PSC/Si-tandem simulations to understand the impact of lateral inhomogeneities, and the interaction with non-ideal measurement conditions such as small-area or non-uniform illumination of the solar cell. We use a tandem addon of the 3D simulation software Quokka3 for our full-cell 3D tandem simulations which treats the perovskite top cell skin, and optionally also the Si bottom cell, with an "equivalent-circuit" model instead of solving the drift-diffusion model. We present simulations and experiments to quantify the impact of inhomogeneous cell properties such as low localized shunt resistances or non-uniformities of the cell absorber, in interaction with the illumination and biasing conditions during the *EQE* measurement. It is specifically interesting to gain insight into lateral effects by simulation, as the experimental investigation of such detailed effects in often metastable PSC/Si tandem cells is highly challenging.
Keywords: Multijunction Solar Cell, Calibration, Simulation, Perovskite, III-V Semiconductors

1 INTRODUCTION

Recently, perovskite/silicon tandem cells (PSC/Si) have shown efficiencies of 31.25% [1] for a lab sized sample and 6" wafer scale PSC/Si have been certified with an efficiency of 26.8 ±1.2 % [2]. At the same time, first commercialization has been announced for the current year, aiming for upscaling size and throughput [3]. In the industrial implementation, processes that have been established for lab-sized cells are in adaptation to high scale output. Compared to small laboratory cells, lateral effects may be more important for full wafer sized cells. This can explain the efficiency decrease seen for perovskite absorbers in the upscaling process [4].

The spatial inhomogeneity has an influence on both, cell performance and the characterization of these cells, e.g., if the methods rely on local illumination only and do not analyse the whole area of the device. This can be critical for *EQE* and *I-V*-characterization, which may lead to significant deviations from the true characteristics and thus to misinterpretations or even misdirected cell development.

To showcase the significance, we examine the impact of lateral effects by the example of local and full illuminating *EQE* measurements both by experiment and simulation. Besides optical lateral non-uniformities which can be expected *e.g.* from non-uniform film thicknesses, we also investigate the impact of a further/more complex electrical *EQE* measurement artifact. This artifact, which is common in two-terminal multi-junction devices, is caused by low shunt resistance (R_{shunt}) or reverse breakdown characteristics [5–7], and depends on the bias voltage and spectral irradiance of the bias illumination.

With the recently released tandem functionality of the 3D solar cell simulation tool Quokka3, we examine how lateral defects such as localized shunts influence this *EQE* artifact.

2 LOCAL *EQE* EFFECTS

2.1 Experimental: Differences between locally and fully illuminated *EQE* measurements

EQE measurements are often performed using monochromatic beam sizes smaller than the actual cell area, mainly due to setup limitations. However, when only one fraction of cell area is chosen for *EQE* characterisation, possible non-uniform optical or electrical cell absorber properties are emphasized or ignored and can possibly lead to results not representative for the whole device.

It is common to calculate the short-circuit current density j_{sc} from measured *EQE*s. Especially for sub-cells of a two-terminal multi-junction device this is not straightforward. j_{sc} determination from *EQE* when measured with a monochromatic light beam smaller than the cell area is influenced by various factors. Obviously, the illumination of a solar cell in a small area can lead to different amounts of shading due to metallization compared to illuminating the whole cell. The same is true for the reference solar cell used for the calibration of the setup.

On the other hand, locally measured EQE neglects possible non-uniform optical or electrical cell absorber properties.

For the investigation we use the *EQE* equipment described in [8], which provides a monochromatic beam of up to more than 6" square in the test plane with low non-uniformity of the bias light (~9.0 %) and, more importantly, of the monochromatic beam (~1.0 %) [9].

As both metastable effects as well as systematic deviations due to local illumination of laterally inhomogeneous samples affect the EQE measurement result, we need to separate both effects. Here, we chose a stable two terminal multi-junction device as a stable test device to exclude meta-stable behaviour which typically is observed for the perovskite top cell.

The sample for investigation is a silicon-based wafer-bonded monolithic triple-junction solar cell

(GaInP/Al$_{0.0635}$GaAs//Si) from a batch with record efficiency (35.9 %) described elsewhere [10, 11].

For the investigation we use a poor sample of the batch (efficiency ~30%) where we observed visible non-uniformity in the top cell´s PL and EL signals (Figure 1).
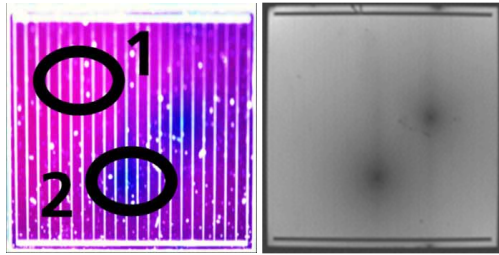

Figure 1: Left: Image of the visible top cell photoluminescence of the III-V//Si sample (2x2 cm²). Circles 1 and 2 indicate the positions of the monochromatic beam in the local-illuminated *EQE* experiments. Right: EL image of the top cell of the same sample.

The *EQE* of all three sub cells was measured with the above mentioned equipment by fully illuminating the whole device and is plotted in Figure 2. The spectral bias irradiance that was used for measuring the top cell is also shown in the graph as areal plots.
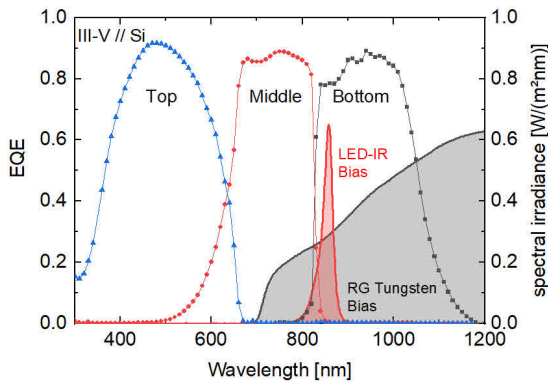

Figure 2: Measured *EQE* of the three sub cells of the investigated III-V//Si sample with full monochromatic illumination as dot line chart. The spectral irradiance of the LED and tungsten bias illumination for top cell limitation is shown as area plot referring to the right Y-axis.

To explore the impact of local *EQE* measurements we illuminated the sample with a monochromatic beam (∅ ~5.8 mm) in two positions as indicated in Figure 1. Position 1 is in a region with high PL signal and position 2 in a region with lower PL signal. The bias light however was illuminating the whole cell area uniformly for all measurements. For both positions *EQE* measurements of the top cell were performed for different bias voltages exploring the above-mentioned artifacts occurring in two terminal devices. The spectral irradiance of the bias illumination was thereby chosen so that the top cell limits the current of the cell (Figure 2).

The results are plotted in the top graph of Figure 3. It can be noted that for the same bias voltage, the absolute *EQE* values differ significantly in the spectral range of absorption of the top cell (~300…640 nm) for the positions 1 and 2.

For the bias voltages below 1.6 V the *EQE* is measured

lower in the wavelength region of interest, whereas an unwanted signal is measured in the wavelength region with no actual response from the investigated sub cell (~640…830 nm), see Figure 3. Interestingly, the height of the artifact signal measured in the spectral range of the middle cell is very similar for positions 1 and 2 of the local *EQE* measurements of the top cell for same bias voltage values.
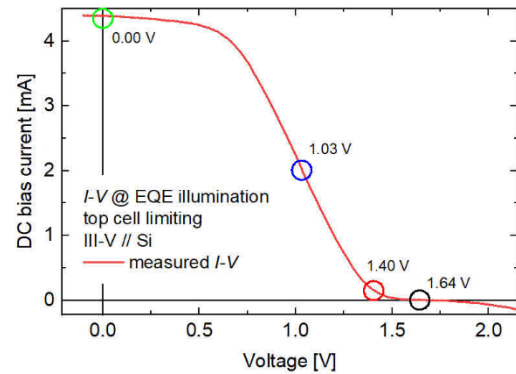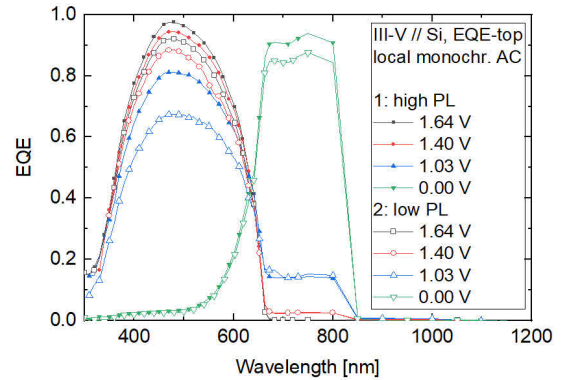

Figure 3: Top: *EQE* measurements with monochromatic light spot (∅ ~5.8 mm) on the 2x2 cm² III-V//Si-sample for different bias-voltages and top cell limiting bias-light at two locations with different PL signal (1 and 2, as in Figure 1). Bottom: *I-V*-sweep performed at *EQE* setup and top cell limiting bias-light. The circles indicate bias voltages used in the *EQE* measurements; their colour coding is used accordingly.

To gain more insight into the artifact behaviour, the lower graph in Figure 3 shows the results of an *I-V*-sweep performed at the *EQE* setup under the same bias illumination as used for the *EQE* measurement of the top cell (Figure 2, right Y-axis).

The different bias voltages used for the *EQE* artifact analysis are shown in the *I-V*-plot as coloured circles. When the bias light irradiance (Figure 2) is used to calculate the current generated in the sub cells, it becomes clear that the photo current of the quasi non-illuminated top cell can be found at ~1.64 V. An early reverse breakdown of the top cell is then observed, and a plateau corresponding to the middle cell current is present at around ~0.00 V. The *I-V*-characteristics can explain how the bias voltage leads to different operating conditions for the *EQE* measurement in dependence of the applied bias voltage: When measuring at 1.64 V, the top cell operates at a (low) current corresponding approximately to its photo current. The measured *EQEs* at this voltage show no artifact signal. For lower bias voltages the multi-junction device is operating in the reverse characteristics of the top

cell. The steep slope leads to an artifact equivalent to a low R_{shunt} as described in [5]. Measurements at 0.00 V show the middle cell *EQE* characteristic which is expected as it is limiting the current at this region of the *I-V*-curve.

The results of the *EQE* measurement when the sample was fully illuminated with the monochromatic beam larger than the cell area are shown in Figure 2. When comparing the maximum *EQE* values of the top cell reached, the fully illuminated *EQE* is similar to the *EQE* values measured locally in the region with low PL signal.

Intuitively the top cell *EQE* measured with full area monochromatic illumination would be expected to show values between the two locally measured *EQE*. However, the influence of the edges on the *EQE* were not covered with the conducted experiment with local monochromatic illumination so that their impact for the 2x2 cm² cell could lead to the observed behaviour of similar *EQE* values for low PL region *EQE* and fully illuminated *EQE*. This underlines the importance of full-area illumination for the determination of accurate *EQE*s.

As a result, it can be stated that local *EQE* measurements can differ significantly depending on the location of the monochromatic light spot. This may lead to erroneous results, especially if *EQE* values are taken to calculate the sub cell j_{sc}s. If j_{sc} values need to be calculated from measured *EQE*s, the tandem device under test should be fully illuminated with monochromatic and spectrally tuned bias light to avoid lateral effects. This requires highly uniform monochromatic and bias light in the measurement plane and careful adjustment of the bias voltage conditions for accurate results.

As stated above, calculated j_{sc} values can be erroneous for different reasons. As a more reliable and proven way to derive absolute *EQE* values for two terminal devices, we advise to perform a spectrometric characterization at a calibrated solar simulator [12, 13].

2.2 Simulations: local R_{shunt} in *EQE* measurement

To analyse the effect of lateral shunts, we use the newly introduced tandem capability [14] of the solar cell simulation software Quokka3 to simulate PSC/Si tandem cells. Briefly, the lumped skin boundary condition to the 3D bulk drift-diffusion solver [15] supports to define *I-V* curves with current generation to represent the perovskite top cell. Two-diode model parameters are accepted for the parameterization of the *I-V* curve, see Figure 4. Thus, local R_{shunt} values can be directly set and varied.
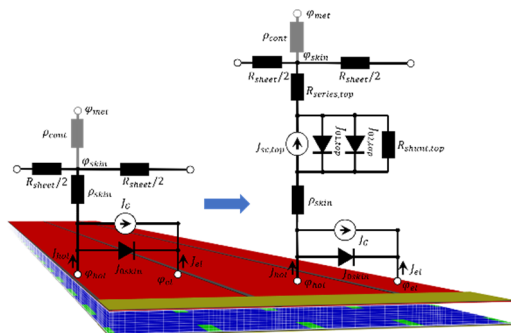

Figure 4: Sketch of Quokka3 tandem concept where the front skin boundary condition is extended to support a top cell *I-V* curve via a 2-diode model.

Optically, the top cell is spectrally defined by its *EQE* and the transmission to the Silicon bottom cell. Both characteristics need to be known from measurements or separate optical modelling. The quasi-analytical treatment of the top cell as a boundary condition results in a similar computational effort compared to single-junction Si cell simulations, which makes large-area 3D tandem cell simulations practically feasible with Quokka3. As several skins can be defined region-wise in Quokka3, it is possible to implement laterally inhomogeneous top cell characteristics, see Figure 5. Different skin regions are connected laterally via the bottom cell, as well as via a sheet resistance representing the front TCO conductive layer, thereby fully accounting for distributed lateral transport effects.

The impact of inhomogeneous cell properties on cell measurements can be understood via 3D modelling. We investigate the case of a significant shunt in the perovskite top cell. The *EQE* measurement procedure of an exemplary PSC/Si tandem cell is simulated in Quokka3: (i) full area bias illumination with a wavelength of 1000 nm is used to "flood" the Si bottom cell, (ii) a terminal voltage corresponding to the V_{oc} of the Si sub cell is applied, and (iii) full area monochromatic illumination of low irradiance and varying wavelength is applied. The resulting incremental current is used to calculate *EQE*.
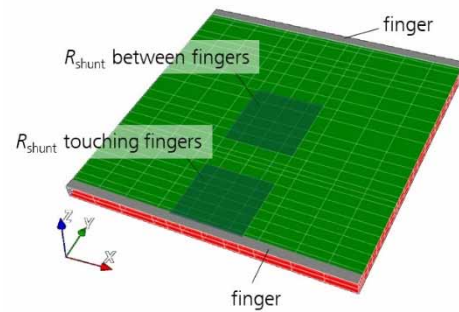

Figure 5: 3D simulation domain in Quokka3 tandem for the analysis of impact of localized shunts.

In an 1D simulation, which represents a uniform cell with homogeneously distributed shunt, we are able to reproduce the effects described by Meusel et al [5], see Figure 6. The main effect of such measurement artifacts is that the *EQE* of another sub cell is measured, while at the same time the signal of the limiting sub cell is too low. In this case the *EQE* of the underlying middle cell is observed.

It is however well known that shunts are rather of localized nature, *e.g.*, occurring at the cell edges or as local defects within the cell area. To represent a localized shunt, we create a 3D solution domain in Quokka3 and confine the shunt only to a small subregion, see Figure 5. We further vary this region by placing it either in the centre between the metal fingers, or touching one of the metal fingers. This is supposed to change lateral transport effects. The local and global R_{shunt} values are chosen so that in each case the shape of the *I-V*-curve under AM1.5g appears to show a similar shunt characteristic, which notably required to choose values somewhat lower than expected from area-averaging (20 Ωcm² for homogeneous case, ~1 Ωcm² for local cases).

The results in Figure 6 (bottom plot) reveal that the localized form of the shunt leads to a smaller *EQE* artifact compared to a homogenous shunt, although the impact on the *I-V* curves is identical. The strength of the effect also

depends on the position of the shunt relative to the metallization. This means that the non-uniformity strongly impacts this *EQE* measurement artifact. Especially the ratio of reduction of measured EQE and the strength of the artifact signal is changed. This ratio is used in the classical correction procedure [6] based on a homogenous assumption. The procedure may therefore be not always correct, when strong influence from local R_{shunt} is present in the respective device under test.
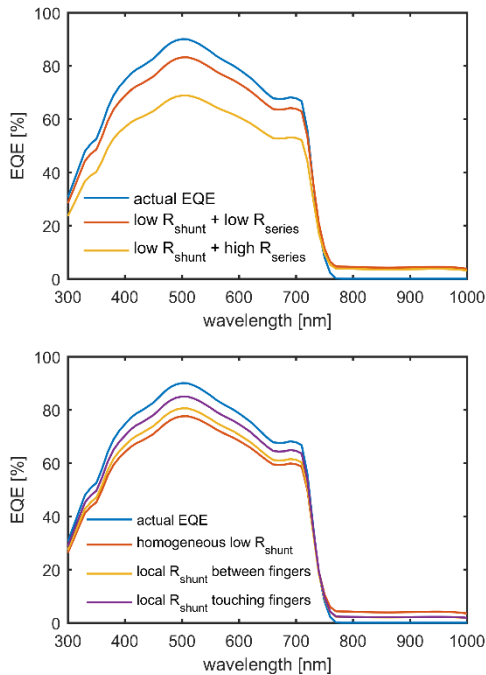

Figure 6: Top: *EQE* artifact resulting from different R_{shunt} and from a combination of R_{shunt} and R_{series}. Bottom: comparison of true *EQE* with 3D simulations for a homogeneous and two local R_{shunt} positions.

3   CONCLUSIONS

The influence on *EQE* measurement of a spatially non-uniform top cell in a two-terminal multi-junction device has been analysed by experiment and simulation. By choosing a III-V//Si-sample for the experiments, the typical metastable behaviour of PSC/Si tandem cells could be avoided, while the non-uniform top cell properties and their impact on *EQE*-characterization in a two-terminal device could be explored.

Two measurements with a monochromatic beam smaller than the cell area have revealed a significantly different *EQE* for the examined top cell. With the light spot in the region of a high PL signal, the *EQE* had higher values compared to the light spot in a region with lower PL signal. This outcome shows that locally measured *EQEs* as it is done by many laboratories can contribute to a non-realistic calculation of the sub cells' j_{sc}s. Instead *EQE* or I_{sc} should be measured using light with high uniformity fully illuminating the device under test (non-uniformity at CalLab PV Cells ~1.0 %, > 6").

During EQE measurement an artifact was observed detected in the spectral region of the middle cell. Apart from the anomalous setting of 0 V, a similar strength for both measurement locations for all applied bias voltages occurred. An *I-V*-sweep recorded under *EQE* bias light

revealed an early breakdown of the limiting top cell. The observed artifact in the *EQE* measurement can therefore be explained with the corresponding reverse characteristic of the limiting top cell. In contrast to the artifact caused by a R_{shunt}, the artifact strength due to reverse breakdown can be reduced to zero when the bias voltage is set close to the photo-current of the limiting top cell (due to the chosen bias illumination here at tandem-V_{oc}). This emphasizes the relevance of bias voltage adjustments.

We further investigated electrical *EQE* measurement artifacts via Quokka3 simulations. For the case of a shunt, which is homogeneously distributed over the entire cell area, the *EQE* results show a behaviour as described with a 1D model from literature.

With 3D simulations the influence of a localized shunt, which is likely more realistic than homogenous shunts in experimental cells, artifact signals in the *EQE*-measurement have been quantified exemplarily. It is shown that both the locality and also the lateral position of the shunt defects have a significant influence on the artifact strength. Additionally, it is observed, that the artifacts caused by local R_{shunt} lead to a different ratio of reduced *EQE* and artifact signal strength as it is known from the artifact caused by homogeneous R_{shunt}. As a consequence, the typical correction procedure for *EQE* measurement artifacts based on the assumption of a uniform R_{shunt} might lead to deviations from the true *EQE* for real experimental tandem cells.

4   ACKNOWLEDGEMENTS

5   REFERENCES

[1] CSEM SA & EPFL, EPFL and CSEM smash through the 30% efficiency barrier for perovskite-on-silicon-tandem solar cells—setting two certified world records: press release, 2022. Accessed: Sep. 21 2022.

[2] M. A. Green et al., "Solar cell efficiency tables (Version 60)," Progress in Photovoltaics: Research and Applications, vol. 30, no. 7, pp. 687–701, 2022, doi: 10.1002/pip.3595.

[3] Oxford PV: press release, 2021.

[4] F. Fu et al., "Monolithic Perovskite-silicon Tandem Solar cells: from the Lab to Fab?," Advanced materials (Deerfield Beach, Fla.), e2106540, 2022, doi: 10.1002/adma.202106540.

[5] M. Meusel, C. Baur, G. Létay, A. W. Bett, W. Warta, and E. Fernandez, "Spectral response measurements of monolithic GaInP/Ga(In)As/Ge triple-junction solar cells: Measurement artifacts and their explanation," Progress in Photovoltaics: Research and Applications, vol. 11, no. 8, pp. 499–514, 2003, doi: 10.1002/pip.514.

[6] G. Siefer, C. Baur, and A. W. Bett, "External quantum

efficiency measurements of Germanium bottom subcells: Measurement artifacts and correction procedures," in 35th IEEE Photovoltaic Specialists Conference (PVSC), 2010: 20-25 June 2010, Honolulu, Hawaii ; conference proceedings, Honolulu, HI, USA, 2010, pp. 704–707.

[7] M. A. Steiner et al., "Measuring IV Curves and Subcell Photocurrents in the Presence of Luminescent Coupling," IEEE J. Photovoltaics, vol. 3, no. 2, pp. 879–887, 2013,
doi: 10.1109/JPHOTOV.2012.2228298.

[8] M. Mundus, "Ultrashort laser pulses for electrical characterization of solar cells," Dissertation, Fraunhofer-Institut für Solare Energiesysteme; Fraunhofer IRB-Verlag, 2016.

[9] M. Mühleis, Spectral Shaping for Accurate Solar Cell Characterization: accepted dissertation, 2022.

[10] R. Müller et al., "Silicon-based monolithic triple-junction solar cells with conversion efficiency > 34%," in Presented at the 37th European PV Solar Energy Conference and Exhibition, 2020, p. 11.

[11] P. Schygulla et al., "Two-terminal III–V//Si triple-junction solar cell with power conversion efficiency of 35.9 % at AM1.5g," Progress in Photovoltaics: Research and Applications, vol. 30, no. 8, pp. 869–879, 2022, doi: 10.1002/pip.3503.

[12] M. Meusel, R. Adelhelm, F. Dimroth, A. W. Bett and W. Warta, "Spectral mismatch correction and spectrometric characterization of monolithic III-V multi-junction solar cells," Progress in Photovoltaics, Vol.10 (2002), No.4, N-17060, 2002,
doi: 10.1002/pip.407.

[13] A. J. Bett et al., "Understanding Sub-Cell Effects and their Influence on the Performance of Monolithic Perovskite/Silicon Tandem Solar Cells: submitted," Adv. Energy Mater., vol. 2022.

[14] A. Fell, O. Schultz-Wittmann, C. Messmer, M. C. Schubert, and S. W. Glunz, "Combining drift-diffusion and equivalent-circuit models for efficient 3D tandem solar cell simulations," IEEE Journal of Photovoltaics, vol. 2022.

[15] A. Fell, J. Schön, M. C. Schubert, and S. W. Glunz, "The concept of skins for silicon solar cell modeling," Solar Energy Materials and Solar Cells, vol. 173, pp. 128–133, 2017,
doi: 10.1016/j.solmat.2017.05.012.